International Journal of Physics and Mathematics
www.physicsjournal.net
Online ISSN: 2664-8644; Print ISSN: 2664-8636
Received: 01-03-2019; Accepted: 03-04-2019; Published: 10-04-2019
Volume 1; Issue 1; January 2019; Page No. 14-24

Second grade Casson fluid flow with variable viscosity and thermal conductivity through a porous medium

Akinpelu FO[1], Alabison RM[2], Olaleye OA[3]
[1] Department of Pure and Applied Mathematics, Ladoke Akintola University (LAUTECH) Ogbomoso, Oyo State, Nigeria
[2-3] Current Address: Department of Mathematics, University of Lagos, Akoka, Yaba, Lagos, Nigeria
[2] Department of Statistics, the Federal Polytechnics, Ede, Osun State, Nigeria

Abstract
This work investigated the convective flow of a second grade Casson fluid through a non-Darcy porous medium under the influence of thermophoresis, Dufour and Soret effects. It is assumed that the viscosity and thermal conductivity are linearly functions of temperature. Similarity transformations were used to reduce the governing partial differential equations (PDE) to a system of nonlinear coupled ordinary differential equations (ODE). Runge Kutta of order four with shooting method was used to obtain the numerical solutions for the velocity, temperature and concentration profiles. The behaviour of the velocity, temperature and concentration distributions was examined using various values of dimensionless numbers like the thermophoresis parameter, τ, at different temperature conditions, porosity parameter Pp, viscoelastic parameter K2 and Prandtl number Pr. τ has no significant effect on velocity and temperature distributions when the heat induced into the system is negligible. Increase in Pp increased the Lorentz force and therefore decreased the velocity but increased the temperature and concentration distributions. Temperature increased with increase in k2 throughout the boundary layer.

Keywords: non-darcy porous medium, second grade casson fluid, runge kutta, thermal conductivity, thermophoresis, viscoelastic

1. Introduction
The study of fluid mechanics is a very important one and has attracted number of scientists over period of time because of its vast area of applications. This includes meteorology (weather forecasting) when some numerical quantitative data about a current state of the atmosphere in an area over a period of time is taken and fluid dynamics and thermodynamics equations are used to estimate and predict what the state of the atmosphere would be in the future. This is widely necessary in agriculture, air-traffic control, military operations, weather alerts, and so on. Furthermore, in turbomachinery, the turbines and compressors are designed in such a way to transfer energy between a rotor and a fluid. Some special fluids which are been studied are also used for various purposes. Such fluids include nanofluids which are used as coolant in engines, electronics and power plants. Ferrofluids are used in medicine. Smart fluids (magnetorheological and electrorheological fluids) whose properties can be changed when magnetic or electric fields are applied are used to reduce vibration in washing machines and air conditioning compressors (Sharma) [1].
In the light of this, Akinbobola and Okoya [2] made a research in the second grade fluid. The flow was over a stretching sheet while the fluid viscosity was made to be inversely linear with temperature. The thermal conductivity was also variable in the presence of heat sink. Their results show that effective cooling will be achieved quickly for viscoelastic fluid with high viscous dissipation because the increasing viscoelastic parameter decreased the temperature. Also, by increasing the value of the Prandtl number, the temperature distribution of the flow region can be reduced. Moreover, Animasaun [3] focused on Casson fluid while he examined the effects of thermophoresis, temperature dependent variable thermal conductivity and fluid viscosity parameters on the fluid. The fluid was in the presence of magnetic field and nth order chemical reaction. He concluded that when temperature dependent fluid viscosity and thermal conductivity is introduced, the velocity of the fluid flow will increase but the temperature and concentration profiles are reduced. In addition, the Casson fluid parameter decreased the temperature and concentration.
Others include, Animasaun *et al.* [4] who used the homotopy analysis method to examine Casson fluid flow along exponentially stretching sheet with variable thermo-physical property, suction and exponentially decaying internal heat generation. Anomalously increased effective thermal conductivities of ethylene glycol-based nanofluids containing copper nanoparticles was studied by Eastman *et al.* [5]. Jia *et al.* [6] worked on entropy generation on MHD Casson nanofluid flow over a porous stretching/shrinking surface. Khan and Pop [7] studied boundary-layer flow of a nanofluid past a stretching sheet. Kuafui and Omar [8] examined applications of Nanofluids in the current and the future of it. Pantokratoras [9] did a numerical reinvestigation into the study of MHD boundary layer flow over a heated stretching sheet with variable viscosity. Over a Nonlinear Stretching sheet with Variable Thickness, Qayyum *et al.* [10] researched about

the chemical reaction and heat generation/absorption aspects in MHD nonlinear convective flow of third grade nanofluid. Rashid *et al.* [11] looked into the aligned magnetic field effects on water based metallic nanoparticles over a stretching sheet with PST and thermal radiation effects. Over a vertical cone with chemical reaction, Reddy *et al.* [12] studied Magnetohydrodynamics natural convection heat and mass transfer of Al_2O_3-water and Ag-water nanofluids. Soomro *et al.* [13] worked on the effects of heat generation/absorption and nonlinear radiation on stagnation point flow of nanofluid along a moving surface.

In view of these literatures and the likes, this work focuses on the second grade Casson fluid flow through a porous medium while the variable viscosity and thermal conductivity are linearly related to the temperature.

2. Mathematical Formulations

The flow is assumed to be two dimensional steady and laminar with viscous incompressible electrically conducting fluid along a porous surface under the influence of Dufour, chemical reaction, viscous dissipation and suction. The Cartesian coordinate system is selected and the assumptions are governed by the following equations:

$$\frac{\partial u}{\partial x}+\frac{\partial v}{\partial y}=0 \tag{1}$$

$$u\frac{\partial u}{\partial x}+v\frac{\partial v}{\partial y}=\frac{1}{\rho}\left(1+\frac{1}{\beta}\right)\frac{\partial \mu_B(T)}{\partial T}\frac{\partial T}{\partial y}\frac{\partial u}{\partial y}+\frac{\mu_B(T)}{\rho}\left(1+\frac{1}{\beta}\right)\frac{\partial^2 u}{\partial y^2}-\frac{\mu_B(T)}{\rho}\left(1+\frac{1}{\beta}\right)\frac{u}{K}$$
$$+g\beta_T(T-T_\infty)+g\beta_C(C-C_\infty)-\frac{b^*}{K}u^2+\frac{\alpha_1}{\rho}\left[\frac{\partial}{\partial x}\left(u\frac{\partial^2 u}{\partial y^2}\right)-\frac{\partial u}{\partial y}\frac{\partial^2 v}{\partial y^2}+v\frac{\partial^3 v}{\partial y^3}\right] \tag{2}$$

$$u\frac{\partial u}{\partial x}+v\frac{\partial v}{\partial y}=\frac{k(T)}{\rho C_p}\frac{\partial^2 T}{\partial y^2}+\frac{1}{\rho C_p}\frac{\partial k(T)}{\partial T}\left(\frac{\partial T}{\partial y}\right)^2+\frac{\mu_B(T)}{\rho C_p}\left(1+\frac{1}{\beta}\right)\left(\frac{\partial u}{\partial y}\right)^2$$
$$+\frac{DK_t}{C_pC_s}\frac{\partial^2 C}{\partial y^2}+\frac{\alpha_1}{\rho C_p}\left[u\frac{\partial u}{\partial y}\frac{\partial^2 u}{\partial x\partial y}+v\frac{\partial u}{\partial y}\frac{\partial^2 u}{\partial y^2}\right] \tag{3}$$

$$u\frac{\partial C}{\partial x}+v\frac{\partial C}{\partial y}+\frac{\partial}{\partial y}\left[V_T(C-C_\infty)\right]=D\frac{\partial^2 C}{\partial y^2}-R^*(C-C_\infty) \tag{4}$$

Subject to:

$$u=Bx \qquad v=-Vx \qquad T=T_w \qquad C=C_w \qquad at \qquad y=0 \tag{5}$$

$$u\to 0 \qquad T\to T_\infty \qquad C\to C_\infty \qquad as \qquad y\to\infty \tag{6}$$

It is assumed that the plastic viscosity $\mu_B(T)$ of the Casson fluid and its thermal conductivity $k(T)$ are linearly related to the temperature as reported by Prasad *et al.* as follows:

$$\mu_B(T)=\mu_B^*\left[\alpha+b(T_w-T)\right] \text{ And } k(T)=k^*\left[\alpha+\gamma(T-T_\infty)\right] \tag{7}$$

Where μ_B^* *and* k^* are constant values of the coefficient of viscosity and thermal conductivity respectively, α , b and γ are constants. $\alpha=1$, $b>0$ And $\gamma>0$.

V_T = thermophoretic velocity parameter = $-\dfrac{K^{Th}}{T_{\mathrm{Re}\,f}}\dfrac{\partial T}{\partial y}$ (8)

Where, K^{Th} = thermophoretic coefficient = $\dfrac{2C_s\left(\lambda_s/\lambda_p + C_t K_n\right)\left[1+K_n\left(C_1 + C_2 e^{-C_3/K_n}\right)\right]}{(1+3C_m K_n)\left(1+2\lambda_s/\lambda_p + 2C_t K_n\right)}$

And τ = thermophoretic parameter for reference temperature = $-\dfrac{K^{Th}(T_w - T_\infty)}{\vartheta T_{\mathrm{Re}\,f}}$

Introducing the following relations for u, v, $\theta(\eta)$ *and* $\phi(\eta)$ as

$$u = \frac{\partial \psi}{\partial x},\ v = -\frac{\partial \psi}{\partial y},\ \theta(\eta) = \frac{T - T_\infty}{T_w - T_\infty},\ \phi(\eta) = \frac{C - C_\infty}{C_w - C_\infty} \tag{9}$$

Substituting equations (7) – (9) into equations (1) – (6) yields

$$\frac{\partial^2 \psi}{\partial x \partial y} - \frac{\partial^2 \psi}{\partial x \partial y} = 0 \tag{10}$$

Thus, equation (1) is satisfied.

$$\begin{aligned}\frac{\partial \psi}{\partial y}\frac{\partial^2 \psi}{\partial x \partial y} - \frac{\partial \psi}{\partial y}\frac{\partial^2 \psi}{\partial y^2} &= -\vartheta^*\left(1+\frac{1}{\beta}\right)\xi\frac{\partial \theta}{\partial y}\frac{\partial^2 \psi}{\partial y^2} + \vartheta^*(1+\xi-\theta\xi)\left(1+\frac{1}{\beta}\right)\frac{\partial^3 \psi}{\partial y^3} \\ &- \frac{\vartheta^*}{K}(1+\xi-\theta\xi)\left(1+\frac{1}{\beta}\right)\frac{\partial \psi}{\partial y} + g\beta_T\theta(T_w - T_\infty) + g\beta_C\phi(C_w - C_\infty) - \frac{b^*}{K}\left(\frac{\partial \psi}{\partial y}\right)^2 \\ &+ \frac{\alpha_1}{\rho}\left[\frac{\partial^2 \psi}{\partial x \partial y}\frac{\partial^3 \psi}{\partial y^3} + \frac{\partial \psi}{\partial y}\frac{\partial^4 \psi}{\partial x \partial y^3} + \frac{\partial^2 \psi}{\partial y^2}\frac{\partial^3 \psi}{\partial x \partial y^2} - \frac{\partial \psi}{\partial x}\frac{\partial^4 \psi}{\partial y^4}\right]\end{aligned} \tag{11}$$

$$\begin{aligned}\frac{\partial \psi}{\partial y}\frac{\partial \theta}{\partial x} - \frac{\partial \psi}{\partial x}\frac{\partial \theta}{\partial y} &= \frac{k^*(1+\theta\varepsilon)}{\rho C_p}\frac{\partial^2 \theta}{\partial y^2} + \frac{k^*\varepsilon}{\rho C_p}\left(\frac{\partial \theta}{\partial y}\right)^2 + \vartheta^*\frac{(1+\xi-\theta\xi)}{(T_w - T_\infty)C_p}\left(1+\frac{1}{\beta}\right)\left(\frac{\partial^2 \psi}{\partial y^2}\right)^2 \\ &+ \frac{DK_t(C_w - C_\infty)}{C_p C_s (T_w - T_\infty)}\frac{\partial^2 \phi}{\partial y^2} + \frac{\alpha_1}{\rho C_p (T_w - T_\infty)}\left[\frac{\partial \psi}{\partial y}\frac{\partial^2 \psi}{\partial y^2}\frac{\partial^3 \psi}{\partial x \partial y^2} - \frac{\partial \psi}{\partial x}\frac{\partial^2 \psi}{\partial y^2}\frac{\partial^3 \psi}{\partial y^3}\right]\end{aligned} \tag{12}$$

$$\frac{\partial \psi}{\partial y}\frac{\partial \phi}{\partial x} - \frac{\partial \psi}{\partial x}\frac{\partial \phi}{\partial y} + \vartheta\tau\phi\frac{\partial^2 \theta}{\partial y^2} + \vartheta\tau\frac{\partial \theta}{\partial y}\frac{\partial \phi}{\partial y} = D\frac{\partial^2 \phi}{\partial y^2} - R^*\phi^n(C_w - C_\infty)^{n-1} \tag{13}$$

Subject to:

$$\frac{\partial \psi}{\partial y} = Bx \qquad \frac{\partial \psi}{\partial x} = V(x) \qquad \theta = 1 \qquad \phi = 1 \qquad at \qquad y = 0 \tag{14}$$

$$\frac{\partial \psi}{\partial y} \to 0 \qquad \theta \to 0 \qquad \phi \to 0 \qquad as \qquad y \to \infty \tag{15}$$

3. Method of Solution

Introducing a similarity variable η and stream function $\psi(x, y)$

$$\eta = y\sqrt{\frac{B}{\vartheta}}, \qquad \psi(x, y) = f(\eta)x\sqrt{\vartheta B} \tag{16}$$

Substituting equation (16) into equations (11) – (15) reduced them to the following set of ordinary differential equation in η .

$$\left(1+\frac{1}{\beta}\right)(1+\xi-\theta\xi)f''' - \xi\left(1+\frac{1}{\beta}\right)\theta' f'' - \left(1+\frac{F_s}{D_a}\right)(f')^2 + ff'' - P_p(1+\xi-\theta\xi)\left(1+\frac{1}{\beta}\right)f' \\ -H_a f' + J_{GR}\xi\theta + J_{GT}\xi\phi + k_2\left(2ff''' + (f'')^2 - ff^{iv}\right) = 0 \tag{17}$$

$$(1+\theta\varepsilon)\theta'' + \varepsilon(\theta')^2 + P_r f\theta' + P_r D_f \phi' + P_r E_c\left[(1+\xi-\theta\xi)\left(1+\frac{1}{\beta}\right)(f'')^2 + k_2\left(f(f'')^2 - ff''f'''\right)\right] = 0 \tag{18}$$

$$\phi'' + S_C f\phi' - \tau S_C \phi\theta'' - \tau S_C \theta'\phi' - S_C k_3 \phi^n = 0 \tag{19}$$

Subject to:

$$f' = 1 \qquad f = s \qquad \theta = 1 \qquad \phi = 1 \qquad at \qquad y = 0 \tag{20}$$

$$f' \to 0 \qquad \theta \to 0 \qquad \phi \to 0 \qquad as \qquad y \to \infty \tag{21}$$

3.1 Numerical Solution

The non-linear coupled ordinary differential equations (170 – (19) subject to the boundary conditions (20) and (21) were solved numerically using Runge-Kutta scheme of order four with shooting method. In order to apply the scheme, the equations were reduced to a set of first order differential equations by using the following transformations.

$$f = f_1 \ , \quad f' = f_2' = f_2 \ , \quad f'' = f_2' = f_3 \ , \quad f''' = f_3' = f_4$$

$$\theta = f_5 \ , \quad \theta' = f_5' = f_6$$

$$\phi = f_7 \ , \quad \phi' = f_7' = f_8$$

$$f_4' = \frac{1}{k_2 f_1}\left[\begin{array}{l}\left(1+\frac{1}{\beta}\right)(1+\xi-f_4\xi)f_4 - \xi\left(1+\frac{1}{\beta}\right)f_6 f_3 - \left(1+\frac{F_S}{D_a}\right)f_2^2 + f_1 f_3 \\ -P_p(1+\xi-f_4\xi)\left(1+\frac{1}{\beta}\right)f_2 + J_{GR}\xi f_5 + J_{GT}\xi f_7 + k_2\left(2f_2 f_4 + f_3^2\right)\end{array}\right] \tag{23}$$

$$f_6' = -\frac{1}{(1+\varepsilon f_5))}\left[\varepsilon f_6^2 + P_r f_1 f_6 + P_r D_7 f_8 + P_r E_C (1+\xi-\xi f_5)\left(1+\frac{1}{\beta}\right) f_3^2 + k_2\left(f_1 f_3^2 - f_1 f_3 f_4\right)\right] \quad (24)$$

$$f_8' = -S_C\left[\tau f_7 f_6' - f_1 f_8 + \tau f_6 f_8 + k_3 f_7\right] \quad (25)$$

Subject to the boundary conditions

$$f_1(0) = S\ ,\ f_2(0) = 1\ ,\ f_5(0) = 1\ ,\ f_4(0) = 1\ ,\ f_7(0) = 1\ ,\ f_2(\infty) \to 0\ ,\ f_5(\infty) \to 0\ ,\ f_7(\infty) \to 0 \quad (26)$$

This was implemented on a computer program written in Matlab.

4. Results and Discussions

The numerical solution obtained from the earlier computer program implementation in Matlab is presented here in graphs and tables and thereafter discussed.

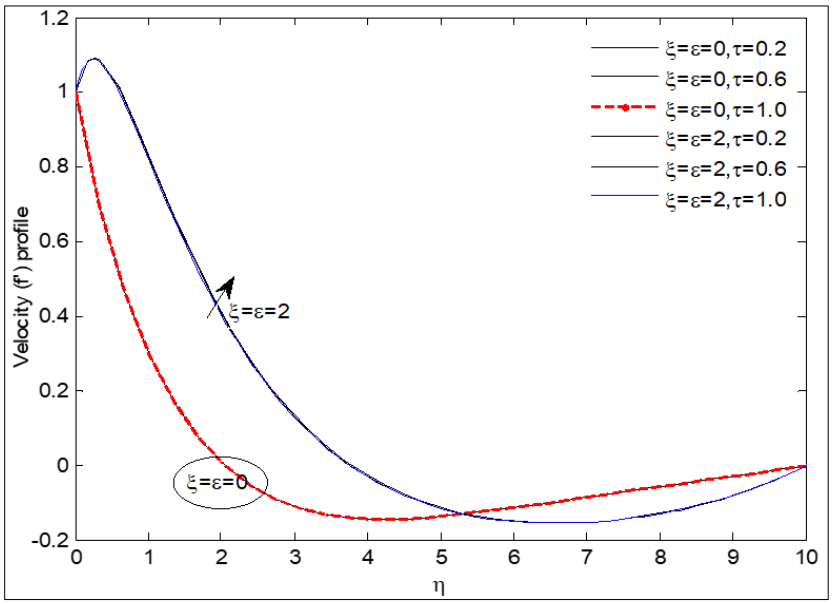

Fig 1: Variation of velocity with thermophoretic(τ), temperature dependent (ξ) and thermal conductivity parameters (ϵ)

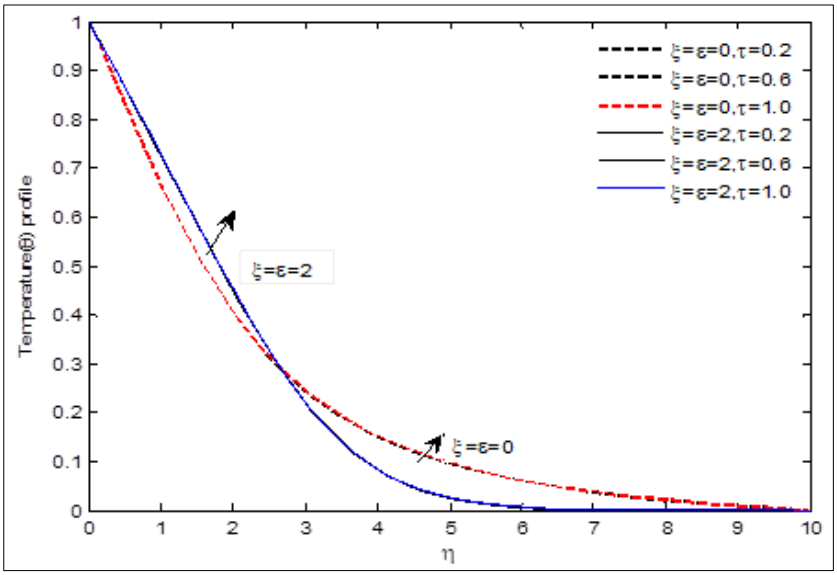

Fig 2: Variation of temperature with thermophoretic(τ), temperature dependent (ξ) and thermal conductivity parameters

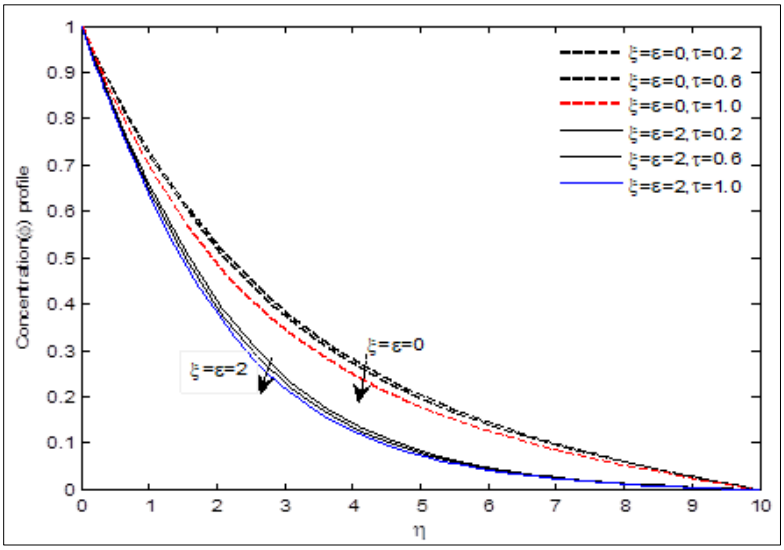

Fig 3: Variation of concentration with thermophoretic(τ), temperature dependent ($\boldsymbol{\xi}$) and thermal conductivity parameters (ϵ)

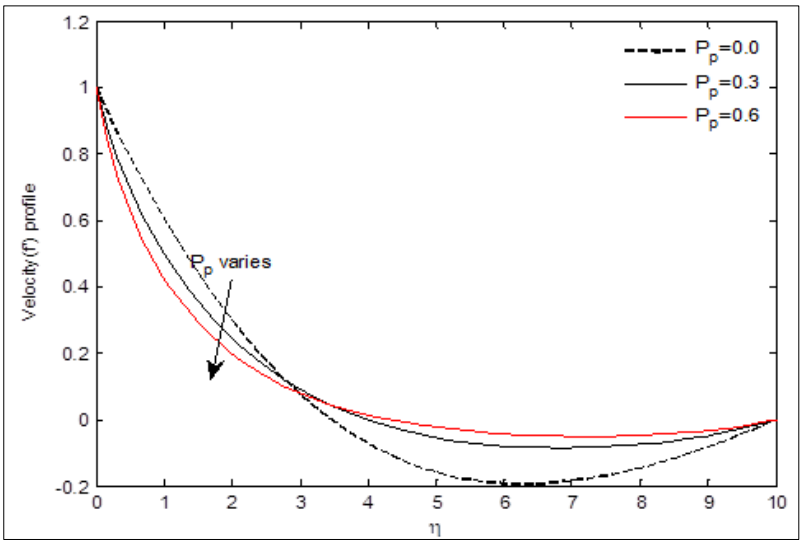

Fig 4: Variation of velocity with Porosity parameter (P_p)

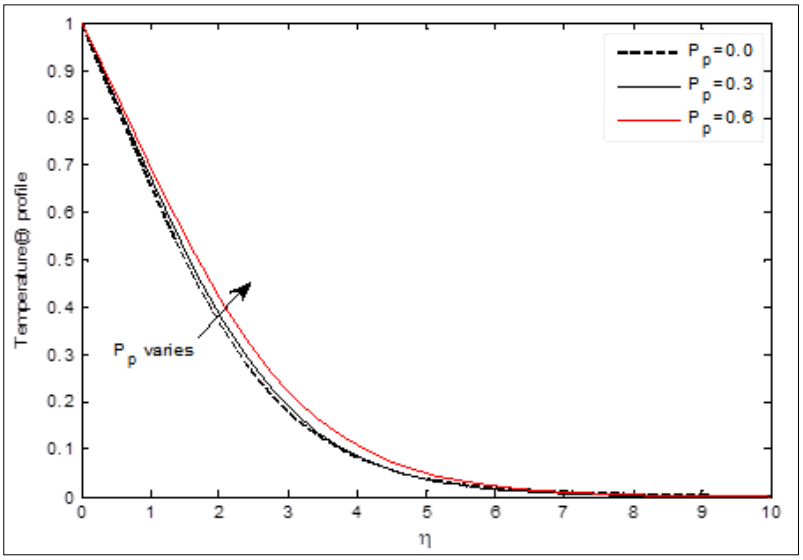

Fig 5: Variation of Temperature with Porosity parameter ***Pp***

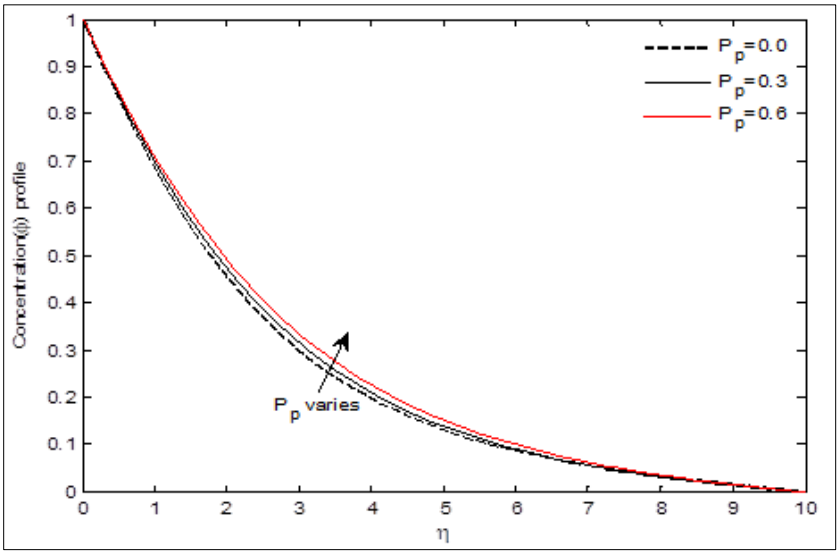

Fig 6: Variation of concentration with porosity parameter (P_p)

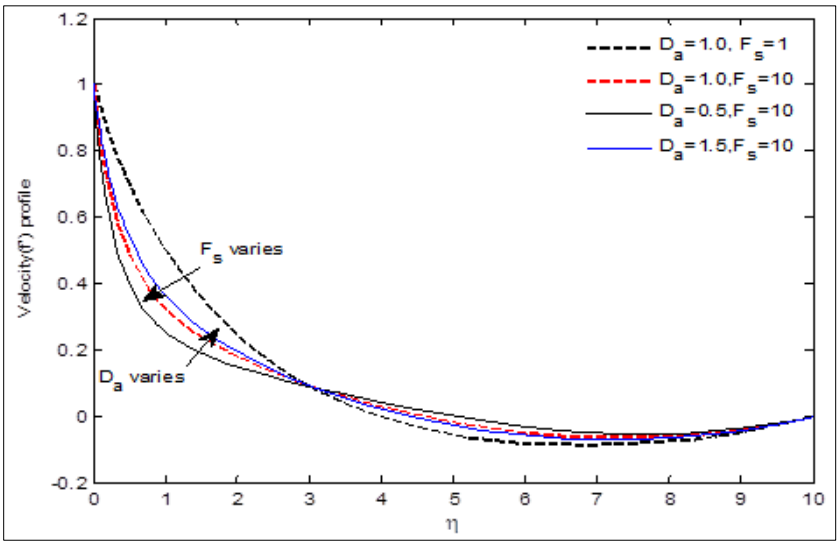

Fig 7: Variation of velocity with Forchheimer (***Fs***) and Darcy (D_a) parameters

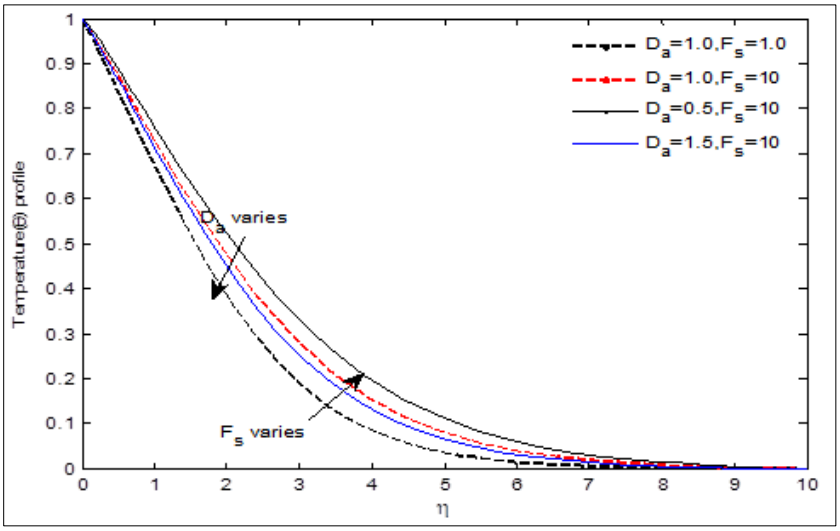

Fig 8: Variation of temperature with Forchheimer (***Fs***) and Darcy (D_a) parameters

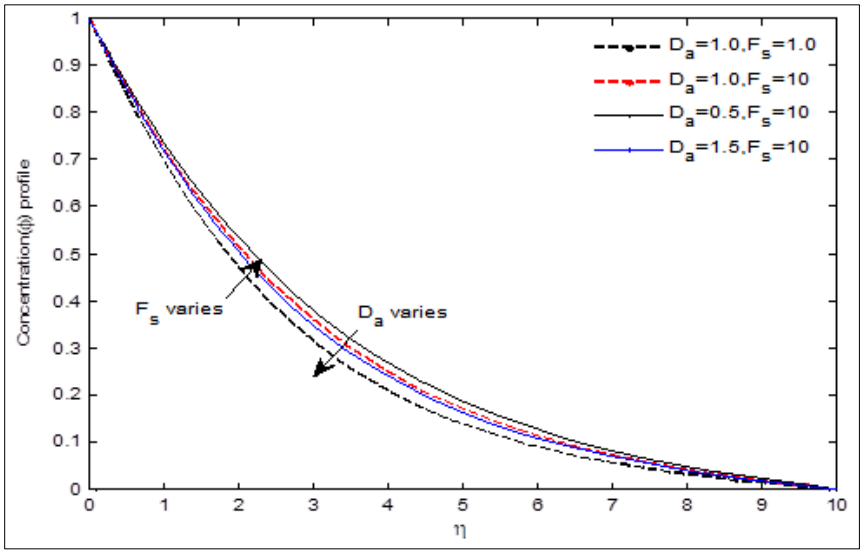

Fig 9: Variation of Concentration with Forchheimer (***Fs***) and Darcy (D_a) parameters

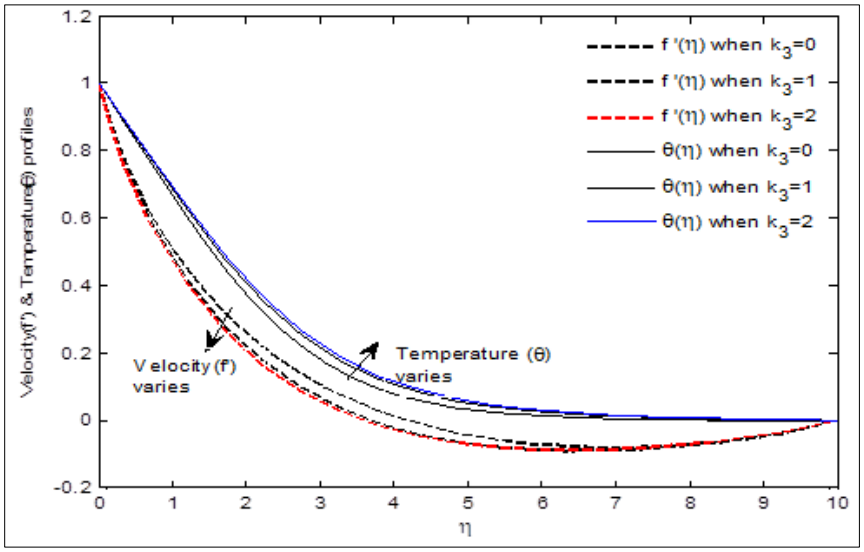

Fig 10: Variation of chemical reaction parameter,, ***k*-3**.. With velocity and Temperature profiles

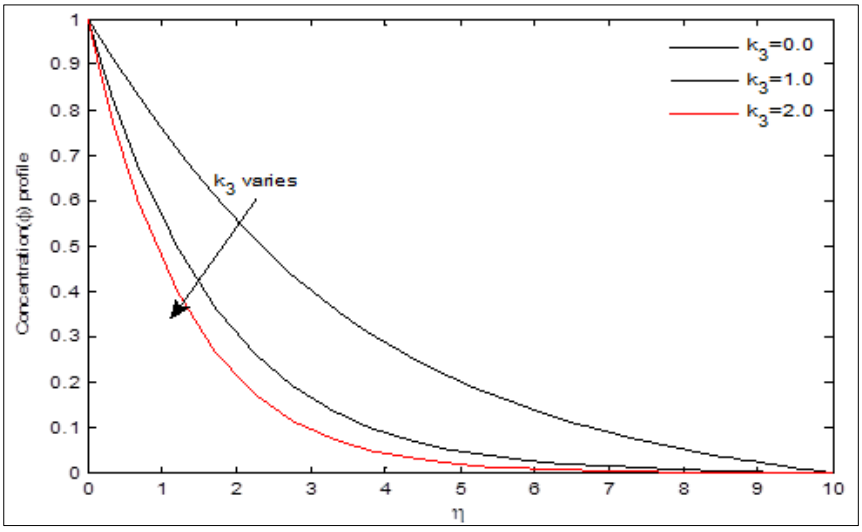

Fig 11: Variation of chemical reaction parameter (k_3) with Concentration

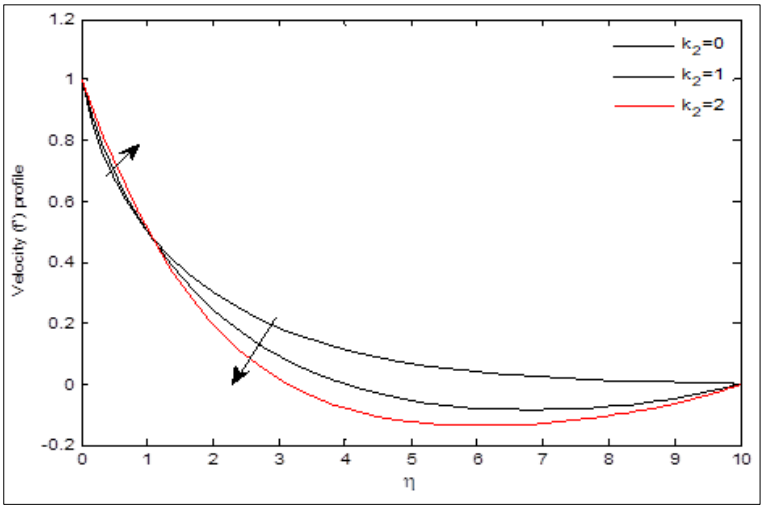

Fig 12: Variation of viscoelastic parameter,, ***k*-2**.. With velocity

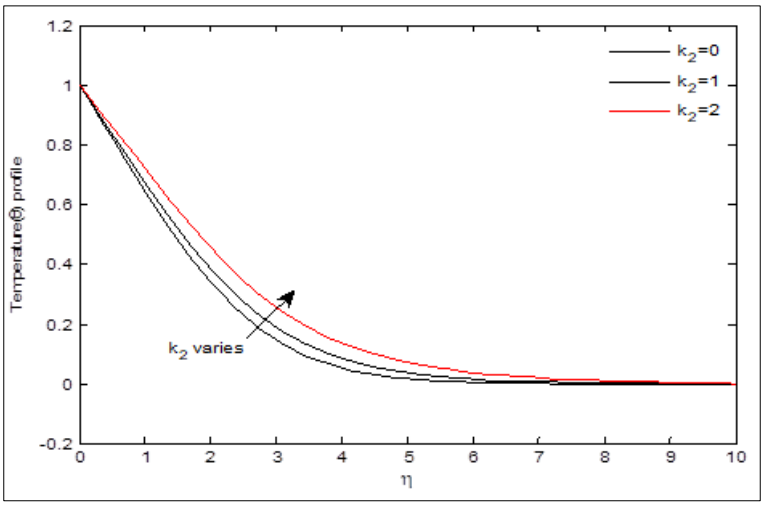

Fig 13: Variation of viscoelastic parameter (k_2) with Temperature

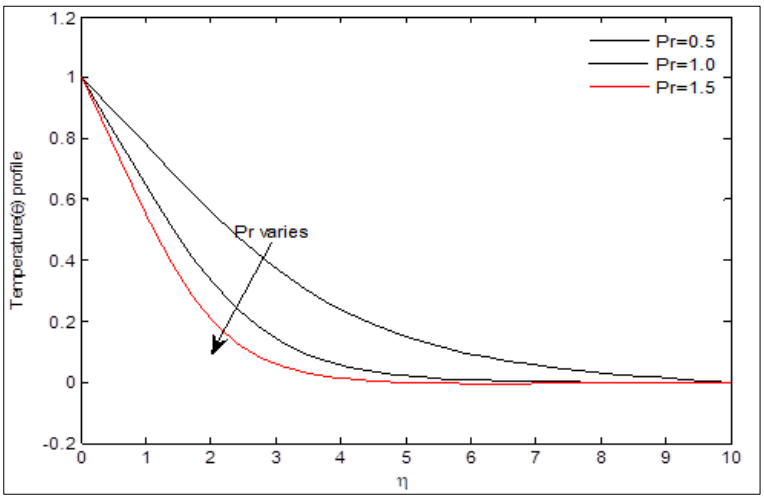

Fig 14: Variation of Prandtl number,, ***P*-r**.. With Temperature

Figures 2 – 4 presents the velocity, temperature and concentration profiles of the flow at different values of τ when heat induced into system is negligible (i.e. $\xi = \varepsilon = 0$) and when the heat is substantial (i.e. $\xi = \varepsilon = 2$). It is noticed that when $\xi = \varepsilon = 0$ and $\xi = \varepsilon = 2$, τ has no significant difference effect on the velocity and temperature distributions. However, the velocity of the flow is

faster when $\xi = \varepsilon = 2$ within the range $0 \le \eta \le 5.4$ and then $\xi = \varepsilon = 0$ within $5.4 \le \eta \le 10$. Also the temperature increase the more with $\xi = \varepsilon = 2$ within $0 \le \eta \le 2.5$. The concentration profile decreased with increase in τ for both $\xi = \varepsilon = 0$ and $\xi = \varepsilon = 2$.

Figures 5 – 7 displayed the effects of the porosity parameter P_p on the velocity, temperature and concentration profiles. It is observed that the velocity deceased with increase in P_p within $0 \le \eta \le 3$ as a result of the dragging force called Lorentz force over the fluid flow which reduced its velocity. The velocity increased with increase in P_p when the drag reduced within $3 < \eta \le 10$. It is also observed that the temperature and concentration profiles increased with increase in P_p. This is because as the porosity increases more heat is introduced into the fluid flow. As a result, the increase in the heat affected the temperature as well as the concentration profiles, hence, the increase in temperature and concentration of the fluid.

Effects of Forchheimer parameter F_s within $0.01 \le F_s \le 10$ and that of Darcy parameter D_a within $0.01 \le D_a \le 2.0$ on the velocity, temperature and concentration were studied in figs. 8 – 10. The velocity increased with increase in F_s within $0 \le \eta \le 2.5$ as a result of increase in the heat within the range. The effect of the heat is negligible outside the range hence the decrease in velocity. Reverse is the case with D_a within the same ranges. The temperature and concentration profiles increased and decreased within F_s and D_a respectively throughout the boundary layer.

In figures 11 and 12, increase in the chemical reaction k_3 depicted a significant effect on the velocity, temperature and the concentration profiles. The velocity and the temperature decreased and increased respectively with k_3. The solutal boundary layer deceased very significantly as k_3 increases.

The effects of the viscoelastic or second grade parameter k_2 on velocity and temperature of the fluid was examined in figures 13 and 14. The velocity increased at the boundary but decreased towards the free stream with increase in k_2 while the temperature increased throughout the boundary layer.

In figure 15, the temperature decrease with increase in the Prandtl number P_r.

5. Conclusion

- Increase in porosity increases the temperature distribution and enhances the heat transport.
- The temperature is however decreased by increasing value of the Prandtl number P_r. Thus P_r reduces the temperature.
- The viscoelastic parameter increases the temperature. Cooling can be effective at lower value of this parameter.
- The presence of the magnetic field produces a dragging force which tends to reduce the heat transport.

6. References

1. Sharma Vishu. Applications of fluid mechanics. Retrieved from: https://www.slideshare.net/VishuSharma13/applications-of-fluid-mechanics-57440275, 2018.
2. Akinbobola Temitope E, Okoya Samuel S. The Flow of Second Grade Fluid over a Stretching Sheet with Variable Thermal Conductivity and Viscosity in the Presence of Heat Source/Sink. Journal of the Nigerian Mathematical Society. 2015; 34:331-342.
3. Animasaun IL. Effects of Thermophoresis, Variable Viscosity and Thermal Conductivity on Free Convective Heat and Mass Transfer of non-Darcian MHD dissipative Casson Fluid flow with Suction and nth order of Chemical Reaction. Journal of the Nigerian Mathematical Society. 2014; 34:11-31.
4. Animasaun IL, Adebile EA, Fagbade AI. Casson fluid flow with variable thermo-physical property along exponentially stretching sheet with suction and exponentially decaying internal heat generation using the homotopy analysis method. Journal of the Nigerian Mathematical Society. 2015; 35:1-17.
5. Eastman JA, Choi SUS, Li S, Yu W, Thompson LJ. Anomalously increased effective thermal conductivities of ethylene glycol-based nanofluids containing copper nanoparticles. Appl Phys Lett. 2001; 78:718-720. Doi: 10.1063/1.1341218.
6. Jia Qing, Muhammad Mubashir Bhatti, Munawwar Ali Abbas, Mohammad Mehdi Rashidi, Mohamed El-Sayed Ali. *et al.*, Entropy Generation on MHD Casson Nanofluid Flow over a Porous Stretching/Shrinking Surface. Entropy, 2016; 18:123. Doi: 10.3390/e18040123.
7. Khan WA, Pop I. Boundary-layer flow of a nanofluid past a stretching sheet. International Journal of Heat and Mass Transfer. 2010; 53:2477-83.
8. Kuafui WV, Omar De Leon. Applications of Nanofluids: Current and Future. Adv Mech Eng, 2010, 519659.
9. Pantokratoras A. Study of MHD Boundary Layer flow over a Heated Stretching Sheet with Variable Viscosity: a Numerical Reinvestigation. International J Heat Mass Transfer. 2008; 51:104-10.

10. Qayyum S, Hayat A, Alsaedi Ahmed. Chemical reaction and Heat Generation/Absorption Aspects in MHD nonlinear Convective Flow of Third Grade Nanofluid over a Nonlinear Stretching sheet with Variable Thickness. Results in Physics. 2017; 7:2752-2761. Doi: http://dx. doi.org/10.1016/j.rinp.2017.07.043.
11. Rashid Irfan, Haq Rizwan Ul, Al-Mdallal Qasem M. Aligned magnetic field effects on water based metallic nanoparticles over a stretching sheet with PST and thermal radiation effects. Phys E. 2017; 89:33-42.
12. Reddy Sudarsana P, Rao KV Suryanarayana. MHD Natural Convection Heat and mass Transfer of Al_2O_3-Water and Ag-Water Nanofluids over a Vertical Cone with Chemical Reaction. Proceedia Engineering. 2015; 127:476-484.
13. Soomro FA, Haq RUl, Al-Mdallal QM, Zhang Q. Heat Generation/Absorption and Nonlinear Radiation Effects on Stagnation point flow of Nanofluid along a moving surface. Results in Physics. 2018; 8:404-414.